

Selected decays of B_s meson in covariant confined quark model

Stanislav Dubnička¹

Anna Zuzana Dubničková²

Mikhail A. Ivanov³

Andrej Liptaj^{1†}

December 18, 2025

¹ Institute of Physics,
Slovak Academy of Sciences, Bratislava, Slovakia.

² Faculty of Mathematics, Physics and Informatics,
Comenius University, Bratislava, Slovakia.

³ Bogoliubov Laboratory of Theoretical Physics,
Joint Institute for Nuclear Research, Dubna, Russia.

† andrej.liptaj@savba.sk

Abstract

We present a study of various B_s meson decays, including hadronic and semileptonic final states with different spins and diagram topologies. The covariant confined quark model is employed to describe hadronic effects, and our analysis serves as a broad test of the current understanding of the underlying dynamics within the Standard Model. The level of agreement with experimental data varies across channels: it is good for the semileptonic decays $B_s^0 \rightarrow D_s^- \mu^+ \nu_\mu$ and $B_s^0 \rightarrow K^- \mu^+ \nu_\mu$; acceptable for the hadronic modes $B_s^0 \rightarrow D_s^- D^+$ and $B_s^0 \rightarrow K^- \pi^+$; marginal for $B_s^0 \rightarrow D_s^- \pi^+$, $B_s^0 \rightarrow D_s^- \rho^+$, and $B_s^0 \rightarrow \phi J/\psi$; and significantly discrepant for $B_s^0 \rightarrow \phi \bar{D}^0$ and $B_s^0 \rightarrow \phi \eta_c$. We argue that the observed inconsistencies may arise from the breakdown of naive factorization and unaccounted long-distance effects. In particular, the channels $B_s^0 \rightarrow D_s^- \pi^+$ and $B_s^0 \rightarrow D_s^- \rho^+$ are theoretically among the cleanest nonleptonic decays, yet they exhibit persistent discrepancies also reported by other theoretical groups.

1 Introduction

Decays of B_s mesons are very rich and include a variety of different spin, flavor and diagram structures. They are usually addressed in some specific context,

our choice to treat them as a whole is mostly data driven. We use the framework of the covariant confined quark model (CCQM) [1] to calculate matrix elements and observables and we have already applied this approach to the B_s particle several times [2, 3, 4, 5, 6, 7]. Nevertheless, since our last text, a quantity of new data on B_s decays appeared and we believe it is appropriate to come back to the subject. These data have different nature and include both, hadronic and semileptonic decays. Specifically, we study the processes

$$\begin{aligned} B_s \rightarrow D_s^- \pi^+, \quad B_s \rightarrow D_s^- \rho^+, \quad B_s \rightarrow D_s^- D^+, \\ B_s \rightarrow K^- \pi^+, \quad B_s \rightarrow \phi \bar{D}^0, \quad B_s \rightarrow \phi \eta_c, \\ B_s \rightarrow D_s^- \mu^+ \nu_\mu, \quad B_s \rightarrow K^- \mu^+ \nu_\mu, \quad B_s \rightarrow \phi e^+ e^-, \end{aligned} \quad (1)$$

all having established branching fractions [8] as measured by [9, 10, 11, 12, 13, 14, 15, 16, 17, 18, 19]. The $B_s \rightarrow K^- \pi^+$ is an analog of $B_s \rightarrow D_s^- D^+$, where the c quark is replaced by the quark of a same type $c \rightarrow u$. For other processes such analogs are not measured (Cabibbo suppressed), but we report their numbers since they follow straightforwardly from our calculations. Namely we give results for

$$\begin{aligned} B_s \rightarrow K^- D^+ & \quad c \leftrightarrow u \text{ in } B_s \rightarrow D_s^- \pi^+, \\ B_s \rightarrow K^- D^{*+} & \quad c \leftrightarrow u \text{ in } B_s \rightarrow D_s^- \rho^+, \\ B_s \rightarrow \phi D^0 & \quad c \leftrightarrow u \text{ in } B_s \rightarrow \phi \bar{D}^0, \\ B_s \rightarrow \phi \pi & \quad c \rightarrow u \text{ in } B_s \rightarrow \phi \eta_c \text{ (factor } 1/2\text{),} \end{aligned}$$

where a factor $1/2$ appears in the last case to reflect the pion quark current structure, where u is mixed with d . We do not reevaluate all other processes addressed in publications mentioned above since we are confident about our model providing consistent results over the time. Nevertheless, some model parameters have slightly shifted, thus we compute $B_s \rightarrow \phi J/\psi$ to compare and cross check.

Besides the “new data” argument, other motivations are present. The performed investigation is a broad test of our weak sector understanding in the Standard Model (SM) and of the CCQM model: predictions we give (as whole) depend on eight Cabibbo-Kobayashi-Maskawa (CKM) matrix elements (all except V_{td}) and predict the relative importance of different flavour-topology amplitudes. Particularly, B_s measurements are complementary to B_d ones: they both have dynamics dominated by a single heavy quark and their comparison may give more insight into penguin contributions and flavor changing neutral current searches. All this has then implications for the parameter determination in the SM and in other theoretical approaches (such as heavy quark effective theory) or for a possible new physics (NP) discovery. The existence of various models on the market with different treatments of hadronic effects is useful to discriminate between the model dependence and the actual physics: if an effect appears throughout most models it may be model independent. In this sense we see our study as relevant.

The processes (1) have been theoretically addressed in several contexts. The $B_s \rightarrow D_s^- \pi^+$ and $B_s \rightarrow D_s^- \rho^+$ reactions get neither penguin nor weak-annihilation contributions and are therefore generally considered as theoretically

clean non-leptonic processes. The former serves as a normalization channel for various other nonleptonic B_s decay modes with a single c quark in the final state, from where the importance to understand it experimentally and theoretically. It was addressed in [20] and [21] to study the factorization, in [22] to probe NP and in other sources too. Explicit numbers for the $D_s^- \rho^+$ final state were given in [23] within the factorization approximation.

The two-charm meson decay $B_s \rightarrow D_s^- D^+$ can be also used to investigate the factorization: from the comparison to analogous beauty baryon decays the importance of non-factorizable effects can be deduced [11]. In addition, when appropriate clean observables are defined, this decay channel may serve for NP searches too, see e.g. [24]. As already mentioned earlier, the $B_s \rightarrow K^- \pi^+$ process is an analog of the latter obtained by $c \rightarrow u$. The theory of charmless B_s decays to light states was addressed multiple times, e.g. in [25, 26], where authors compute branching fractions, CP-violating asymmetries and discuss NP effects, or in [27] where the subject is the weak phase $\gamma \equiv \text{Arg}(V_{ub}^*)$ determination. The reference [28] then focuses on further corrections (to mesonic wave function and distribution amplitudes) of this decay.

The $B_s \rightarrow \phi \bar{D}^0$ process (see e.g. [29, 30, 31]) is generally seen as complementary to other B_s and B_d decays, possibly improving constraints on various weak physics parameters.

The last non-leptonic process we consider is $B_s \rightarrow \phi \eta_c$. The authors of the reference [32] use this decay to determine the $B_s \rightarrow \phi$ matrix element, then argue about the implications for $f(980)$, which they claim to be a tetraquark. The work [33] investigates various $B_s \rightarrow \eta_c h$ transitions including known next-to-leading order (NLO) contributions. The authors demonstrate that these have an important effect.

Semileptonic decays are significantly more theoretically clean and consequently more precisely predicted and more discussed. The decays $B_s \rightarrow D_s^- \mu^+ \nu_\mu$ and $B_s \rightarrow K^- \mu^+ \nu_\mu$ allow to determine V_{cb} and V_{ub} elements and their ratio from exclusive processes and in this sense they constraint NP searches. They provide complementary information to B_d processes, the presence of the heavier valence quark s may benefit to lattice quantum chromodynamics (QCD) calculations by providing smaller statistical errors and finite-volume effects [34]. A large body of literature dealing with these decays can be cited, such as [35, 36, 37, 38, 39] and [40, 41, 42, 38, 43], with the lattice QCD starting to dominate in theoretical evaluations.

The decay $B_s \rightarrow \phi^0 e^+ e^-$ is a $\bar{b} \rightarrow \bar{s}$ flavor-changing neutral current process which, in the SM, proceeds only via loops. This makes of it a natural candidate for NP searches: hypothetical new particles can enter the loop and modify the amplitude. The muon version was measured already a time ago [44] and some theory-experiment tensions appeared [45] (true also for $B \rightarrow K^{(*)} \mu^+ \mu^-$). The $e^+ e^-$ decay represents a consistency test with respect to its $\mu^+ \mu^-$ counterpart and, on the same footing, is interesting as NP and lepton universality probe. Most literature does not differentiate and works with a general dilepton $\ell \bar{\ell}$ in the final state, e.g. [46].

As stated already, we use the covariant confined quark model as a tool to

describe processes which include hadrons. The CCQM is an enhanced effective-theory model that unifies covariance, gauge interactions and quark confinement while keeping the number of free parameters limited. It is based on a non-local interaction Lagrangian where quark-hadron interaction vertex is introduced, allowing a hadron to turn into its constituent quarks and vice versa. Then, on the quark level, we work with effective four fermion operators. Acknowledging the impressive progress in methods with small model dependence (in particular the lattice QCD), we consider quark models as a more versatile and valid complements. We describe the CCQM in more detail later in a dedicated section.

The text is structured as follows: first, we present the general theory of weak decays formulated in terms of effective Hamiltonians, hadronic form factors and decay constants. Next, we present the CCQM and its basic features, coming next to our results and conclusion. The theoretical content we need to cover is large, therefore we keep out text concise and provide only essential information with numerous references to our previous works, where details can be found.

2 Theory

2.1 Weak decays in effective theory

Weak decays of hadrons proceed, on the quark level, through weak decays of valence quarks. The transition from the initial state fermions to the final state fermions involves various Feynman diagrams which however need not to be reevaluated for every calculation. Effectively, one can define a small number of (four-fermion) operators and weight their action by (scale dependent) Wilson coefficients. A given operator integrates contributions from various diagrams and several theoretical groups dedicate their work to evaluate them and find the value of the corresponding Wilson coefficient. The number of effective operators is given by the Lorentz, chiral and color structure of the connected particles (fermions). The choice of operators depends on the underlying process and we will not list operator sets for all cases we address, because this is a well-known model-independent framework described in details in [47]. Nevertheless it seems appropriate to illustrate the effective approach on a model example. We choose the $B_s \rightarrow \phi^0 e^+ e^-$ decay which is rich in contributing operators. For this process the effective Hamiltonian is written

$$B_s \rightarrow \phi^0 e^+ e^- : \quad \mathcal{H}_{\text{eff.}} = -\frac{4G_F}{\sqrt{2}} \lambda_t \sum_{i=1}^{10} C_i(\mu) \mathcal{O}_i(\mu) \quad (2)$$

with

$$\begin{aligned}
\mathcal{O}_1 &= (\bar{s}_{a_1} \gamma^\mu P_L c_{a_2}) (\bar{c}_{a_2} \gamma_\mu P_L b_{a_1}), & \mathcal{O}_2 &= (\bar{s} \gamma^\mu P_L c) (\bar{c} \gamma_\mu P_L b), \\
\mathcal{O}_3 &= (\bar{s} \gamma^\mu P_L b) \sum_q (\bar{q} \gamma_\mu P_L q), & \mathcal{O}_4 &= (\bar{s}_{a_1} \gamma^\mu P_L b_{a_2}) \sum_q (\bar{q}_{a_2} \gamma_\mu P_L q_{a_1}), \\
\mathcal{O}_5 &= (\bar{s} \gamma^\mu P_L b) \sum_q (\bar{q} \gamma_\mu P_R q), & \mathcal{O}_6 &= (\bar{s}_{a_1} \gamma^\mu P_L c_{a_2}) \sum_q (\bar{q}_{a_2} \gamma_\mu P_R q_{a_1}), \quad (3) \\
\mathcal{O}_7 &= \frac{e}{16\pi^2} \bar{m}_b (\bar{s} \sigma^{\mu\nu} P_R b) F_{\mu\nu}, & \mathcal{O}_8 &= \frac{g}{16\pi^2} \bar{m}_b (\bar{s} \sigma^{\mu\nu} P_R \mathbf{T}_{a_1 a_2} b_{a_2}) \mathbf{G}_{\mu\nu}, \\
\mathcal{O}_9 &= \frac{e}{16\pi^2} (\bar{s} \gamma^\mu P_L b) (\bar{\ell} \gamma_\mu \ell), & \mathcal{O}_{10} &= \frac{e}{16\pi^2} (\bar{s} \gamma^\mu P_L b) (\bar{\ell} \gamma_\mu \gamma_5 \ell).
\end{aligned}$$

The symbol G_F denotes the Fermi coupling constant, λ_t the product of the CKM elements $\lambda_t = |V_{tb} V_{ts}^*|$, $\sigma^{\mu\nu} = \frac{i}{2} [\gamma^\mu, \gamma^\nu]$, $C_i(\mu)$ are renormalization-scale μ dependent Wilson coefficients and \mathcal{O}_i the effective operators. These are built from quark fields (s, c, b and q) which carry color subscript a_i , shown only for nontrivial combinations. Further $P_{L/R} = (1 \mp \gamma_5)/2$, \bar{m}_b is the QCD bottom quark mass (different from the constituent quark mass of the CCQM), $F_{\mu\nu}$ is the electromagnetic tensor, $\mathbf{G}_{\mu\nu}$ the gluon field strength tensor and $\mathbf{T}_{a_1 a_2}$ are the generators of the color $SU(3)$ group. Operators $\mathcal{O}_{1,2}$ are referred to as current-current, \mathcal{O}_{3-6} as QCD penguins, $\mathcal{O}_{7,8}$ are labeled “magnetic penguin” and $\mathcal{O}_{9,10}$ as electroweak penguins. All these are then used to express the decay amplitude through Wilson coefficients and transition amplitudes $B_s \rightarrow \phi$. Using hadronic form factors to parameterize the latter, one gets the final formula for the amplitude and the decay with. We avoid writing the expression here because of its length, the reader can find it in references [48, 49, 5].

2.2 Hadronic form factors

Assuming the naïve factorization, the amplitude splits into the product of a hadronic transition amplitude and a leptonic decay constant (for hadronic decays) or a leptonic vector (for semi-leptonic decays). The transition amplitude is then parameterized by form factors which appear as scalar q^2 -dependent coefficients in front of independent Lorentz structures. With B_s a pseudoscalar particle (denoted as P , a vector particle as V), we deal only with a small number of hadronic transition amplitudes. The definition of form factors then stands

$$(P = p_1 + p_2, q = p_1 - p_2)$$

$$\begin{aligned}
(P'P)_V &= \left\langle P'_{[\bar{q}_3 q_2]}(p_2) | \bar{q}_2 \gamma^\mu q_1 | P_{[\bar{q}_3 q_1]}(p_1) \right\rangle = F_+(q^2) P^\mu + F_-(q^2) q^\mu, \\
(P'P)_S &= \left\langle P'_{[\bar{q}_3 q_2]}(p_2) | \bar{q}_2 q_1 | P_{[\bar{q}_3 q_1]}(p_1) \right\rangle = (m_{P'} + m_P) F_S(q^2), \\
(VP)_V &= \left\langle V_{[\bar{q}_3 q_2]}(p_2, \epsilon) | \bar{q}_2 \gamma^\mu (1 - \gamma_5) q_1 | P_{[\bar{q}_3 q_1]}(p_1) \right\rangle = \frac{\epsilon_\nu^\dagger}{m_P + m_V} \\
&\quad \times \left[-g^{\mu\nu} (P \cdot q) A_0(q^2) + P^\mu P^\nu A_+(q^2) + q^\mu P^\nu A_-(q^2) + i \varepsilon^{\mu\nu\alpha\beta} P_\alpha q_\beta V(q^2) \right], \\
(VP)_T &= \left\langle V_{[\bar{q}_3 q_2]}(p_2, \epsilon) | \bar{q}_2 \sigma^{\mu\nu} q_\nu (1 + \gamma_5) q_1 | P_{[\bar{q}_3 q_1]}(p_1) \right\rangle = \epsilon_\nu^\dagger \left[- \left(g^{\mu\nu} - \frac{q^\mu q^\nu}{q^2} \right) \right. \\
&\quad \left. \times (P \cdot q) a_0(q^2) + \left(P^\mu P^\nu - \frac{q^\mu P^\nu (P \cdot q)}{q^2} \right) a_+(q^2) + i \varepsilon^{\mu\nu\alpha\beta} P_\alpha q_\beta q(q^2) \right], \tag{4}
\end{aligned}$$

where we list form factors relevant for our calculations. To complete the model example from the previous section, the $B_s \rightarrow \phi^0 e^+ e^-$ matrix element is expressed as

$$\begin{aligned}
\mathcal{M} &= \frac{G_F \alpha \lambda_t}{\sqrt{2} 2\pi} \left\{ C_9^{\text{eff.}} \mathcal{M}_1^\mu (\bar{e} \gamma_\mu e) - \frac{2 \bar{m}_b}{q^2} C_7^{\text{eff.}} \mathcal{M}_2^\mu (\bar{e} \gamma_\mu e) + C_{10} \mathcal{M}_1^\mu (\bar{e} \gamma_\mu \gamma_5 e) \right\}, \\
\mathcal{M}_1^\mu &= \langle \phi | \bar{s} \gamma^\mu (1 - \gamma_5) b | B_s \rangle, \\
\mathcal{M}_2^\mu &= \langle \phi | \bar{s} i \sigma^{\mu\nu} q_\nu (1 + \gamma_5) b | B_s \rangle,
\end{aligned}$$

with

$$\begin{aligned}
C_7^{\text{eff.}} &= C_7^{\text{eff.}} (C_5, C_6, C_7), \\
C_9^{\text{eff.}} &= C_9^{\text{eff.}} (C_1, C_2, C_3, C_4, C_5, C_6, C_9)
\end{aligned}$$

being some known, specific function of Wilson coefficients from (2), see [5], and α is the electromagnetic (EM) coupling. The amplitudes $\mathcal{M}_{1,2}^\mu$ are parameterized as given by (4).

To express the decay widths we use intermediate objects, the helicity form

factors, which are defined as

$P \rightarrow P :$

$$H_t = \frac{1}{\sqrt{2}} \left[(m_P^2 - m_{P'}^2) F_+ + q^2 F_- \right],$$

$$H_0 = \frac{2m_P |\mathbf{p}_2|}{\sqrt{q^2}} F_+,$$

$P \rightarrow V :$

$$H_t = \frac{1}{m_P + m_{P'}} \frac{m_P}{m_{P'}} \frac{|\mathbf{p}_2|}{\sqrt{q^2}} \left[(m_P^2 - m_{P'}^2) (A_+ - A_0) + q^2 A_- \right],$$

$$H_{\pm} = \frac{1}{m_P + m_{P'}} \left[- (m_P^2 - m_{P'}^2) A_0 \pm 2m_P |\mathbf{p}_2| V \right],$$

$$H_0 = \frac{1}{m_P + m_{P'}} \frac{1}{2m_{P'} \sqrt{q^2}} \left[- (m_P^2 - m_{P'}^2) (m_P^2 - m_{P'}^2 - q^2) A_0 + 4m_P^2 |\mathbf{p}_2|^2 A_+ \right],$$

where $|\mathbf{p}_2|$ is the absolute value of the three-momentum of outgoing particles in the B_s rest frame and can be expressed through the Källén λ function $|\mathbf{p}_2| = \sqrt{\lambda(m_P^2, m_{P'}^2, q^2)/(2m_P)}$. The $P \rightarrow V$ tensor form factors a_0 , a_+ and q appear only for $B_s \rightarrow \phi^0 e^+ e^-$, we comment on them in the result section.

2.3 Decay widths

We provide here the list of decay-width formulas, all of which can be found in the literature or our previous publications (see e.g. Appendix A in [50]). For each formula we list the relevant processes and show Feynman diagrams. When dealing with hadronic decays we refer to different diagram topologies as class 1 (color allowed) or class 2 (color suppressed). Letters a_i and $C_X^{(\text{eff.})}$ denote combinations of the Wilson coefficients

$$a_1 = C_2 + \xi C_1,$$

$$a_2 = C_1 + \xi C_2,$$

$$C_2^{\text{eff.}} = C_2 + \xi C_1 + C_4 + \xi C_3,$$

$$C_6^{\text{eff.}} = C_6 + \xi C_5,$$

$$C_P = C_1 + \xi C_2 + C_3 + \xi C_4 - C_5 - \xi C_6,$$

$$C_V = C_1 + \xi C_2 + C_3 + \xi C_4 + C_5 + \xi C_6,$$

where $\xi = 1/N_c$ with N_c being the number of colors and f_M denotes the leptonic decay constant of the meson M (f_M^S is the scalar decay constant related to the scalar form factor F_S).

2.3.1 Class 1, $PS \rightarrow PS + PS$

Included decays: $B_s^0 \rightarrow D_s^- \pi^+$

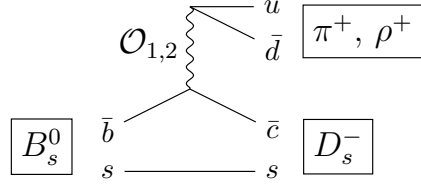


Figure 1: The feynman diagram of decays $B_s^0 \rightarrow D_s^- + \pi^+$ and $B_s^0 \rightarrow D_s^- + \rho^+$.

Contributing operators: $\mathcal{O}_1, \mathcal{O}_2$

Decay width formula:

$$\Gamma(B_s^0 \rightarrow D_s^- \pi^+) = \frac{1}{16\pi m_{B_s}^2} |\mathbf{p}_2| G_F^2 (V_{cb} V_{ud})^2 \left[a_1 f_\pi m_\pi H_t^{B_s \rightarrow D_s}(m_\pi^2) \right]^2$$

Diagram: Figure 1.

2.3.2 Class 1, $PS \rightarrow PS + V$

Included decays: $B_s^0 \rightarrow D_s^- \rho^+$

Contributing operators: $\mathcal{O}_1, \mathcal{O}_2$

Decay width formula:

$$\Gamma(B_s^0 \rightarrow D_s^- \rho^+) = \frac{1}{16\pi m_{B_s}^2} |\mathbf{p}_2| G_F^2 (V_{cb} V_{ud})^2 \left[a_1 f_\rho m_\rho H_0^{B_s \rightarrow D_s}(m_\rho^2) \right]^2$$

Diagram: Figure 1.

2.3.3 Class 1 + penguin, $PS \rightarrow PS + PS$

Included decays: $B_s^0 \rightarrow D_s^- D^+$, $B_s^0 \rightarrow K^- \pi^+$

Contributing operators: $\mathcal{O}_1, \dots, \mathcal{O}_6$

Decay width formula:

$$\begin{aligned} \Gamma(B_s^0 \rightarrow D_s^- D^+) = & \frac{1}{16\pi m_{B_s}^2} |\mathbf{p}_2| G_F^2 (V_{cb} V_{cd})^2 \\ & \times \left[C_2^{\text{eff}} f_D m_D H_t^{B_s \rightarrow D_s}(m_D^2) + 2C_6^{\text{eff}} f_D^S F_S^{B_s \rightarrow D_s}(m_D^2) \right]^2 \end{aligned}$$

Diagram: Figure 2.

2.3.4 Class 2, $PS \rightarrow V + PS$

Included decays: $B_s^0 \rightarrow \phi \overline{D^0}$

Contributing operators: $\mathcal{O}_1, \mathcal{O}_2$

Decay width formula:

$$\Gamma(B_s^0 \rightarrow \phi \overline{D^0}) = \frac{1}{16\pi m_{B_s}^2} |\mathbf{p}_2| G_F^2 (V_{cb} V_{us})^2 \left[a_2 f_{\overline{D^0}} m_{\overline{D^0}} H_t^{B_s \rightarrow \phi}(m_{\overline{D^0}}^2) \right]^2$$

Diagram: Figure 3.

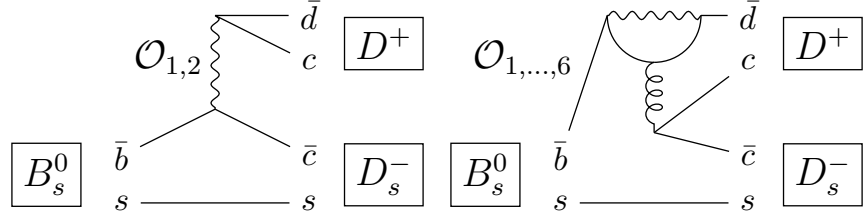


Figure 2: The Feynman diagrams of the decay $B_s^0 \rightarrow D_s^- + D^+$.

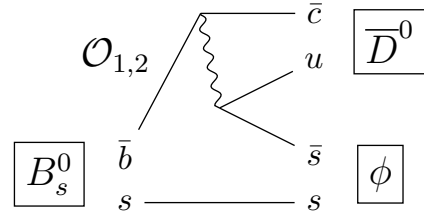


Figure 3: The Feynman diagram of the decay $B_s^0 \rightarrow \phi + \bar{D}^0$.

2.3.5 Class 2 + penguin, $PS \rightarrow V + PS$

Included decays: $B_s^0 \rightarrow \phi \eta_c$, $B_s^0 \rightarrow \phi \pi$
 (additional factor 1/2 in the decay width with the pion)
 Contributing operators: $\mathcal{O}_1, \dots, \mathcal{O}_6$
 Decay width formula:

$$\Gamma(B_s^0 \rightarrow \phi \eta_c) = \frac{G_F^2}{16\pi} \frac{|\mathbf{p}_2|}{m_{B_s}^2} |V_{cb} V_{cs}^\dagger|^2 \left[C_P f_{\eta_c} m_{\eta_c} H_t^{B_s \rightarrow \phi} (m_{\eta_c}^2) \right]^2$$

Diagram: Figure 4.

2.3.6 Class 2 + penguin, $PS \rightarrow V + V$

Included decays: $B_s^0 \rightarrow \phi + J/\psi$
 Contributing operators: $\mathcal{O}_1, \dots, \mathcal{O}_6$

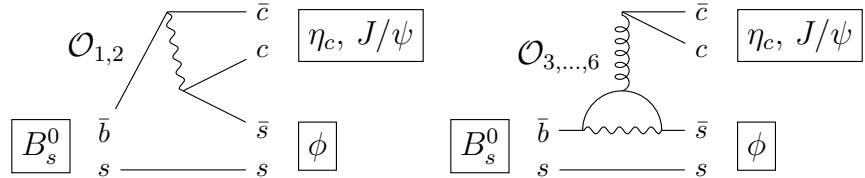


Figure 4: The Feynman diagrams of decays $B_s^0 \rightarrow \phi + \eta_c$ and $B_s^0 \rightarrow \phi + J/\psi$.

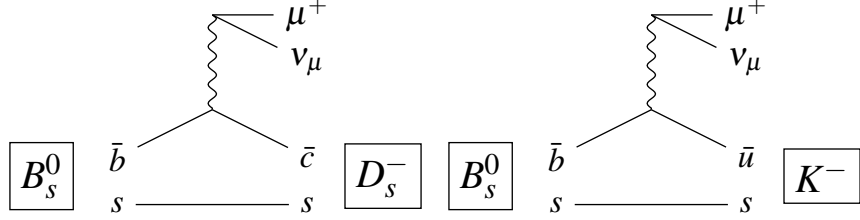


Figure 5: The Feynman diagrams of decays $B_s^0 \rightarrow D_s^- + \mu^+ \nu$ and $B_s^0 \rightarrow K^- + \mu^+ \nu$.

Decay width formula:

$$\Gamma(B_s^0 \rightarrow \phi J/\psi) = \frac{G_F^2}{16\pi} \frac{|\mathbf{p}_2|}{m_{B_s}^2} |V_{cb} V_{cs}^\dagger|^2 C_V^2 f_{J/\psi}^2 m_{J/\psi}^2 \sum_{i=0,\pm} \left[H_i^{B_s \rightarrow \phi} (m_{J/\psi}^2) \right]^2$$

Diagram: Figure 4.

2.3.7 Semileptonic, with neutrino, $PS \rightarrow PS + \mu^+ \nu$

Included decays: $B_s^0 \rightarrow D_s^- \mu^+ \nu$, $B_s^0 \rightarrow K^- \mu^+ \nu$

Decay width formula:

$$\begin{aligned} \Gamma(B_s^0 \rightarrow D_s^- \mu^+ \nu) &= \frac{G_F^2 |V_{cb}|^2}{(2\pi)^3} \\ &\times \int_{m_\mu}^{(m_{B_s} - m_{D_s})^2} \frac{(q^2 - m_\mu^2)}{12m_{B_s}^2 q^2} |\mathbf{p}_2| \left[\left(1 + \frac{m_\mu^2}{2q^2} \right) H_0^2 + \frac{3m_\mu^2}{2q^2} H_t^2 \right] dq^2 \end{aligned}$$

Diagram: Figure 5.

2.3.8 Semileptonic, with dilepton, $PS \rightarrow V + \ell^+ \ell^-$

Included decays: $B_s^0 \rightarrow \phi^0 e^+ e^-$

Decay width formula:

$$\Gamma(B_s^0 \rightarrow \phi^0 e^+ e^-) = \int dq^2 \frac{G_F^2}{(2\pi)^3} \frac{\alpha^2 |V_{tb} V_{ts}^*|^2}{(2\pi)^2} \frac{|\mathbf{p}_2| q^2 \beta_e}{12m_{B_s}^2} H_{\text{tot}},$$

where $\beta_e = \sqrt{1 - 4m_e^2/q^2}$ and H_{tot} is function of invariant form factors and Wilson coefficients $H_{\text{tot}} = H_{\text{tot}}(A_\pm, A_0, V, a_0, a_+, g, C_{1,\dots,10})$ whose explicit form can be found in [5].

Diagram: Figure 6.

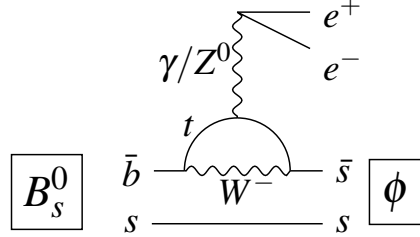


Figure 6: The Feynman diagram of the decay $B_s^0 \rightarrow \phi^0 e^+ e^-$.

3 Model

3.1 Formulation

The role of the CCQM model is to predict the invariant form factors and leptonic decay widths. These objects enclose also contributions from non-perturbative hadronic effects related to B_s not being elementary, but being rather a bound state of strongly interacting quarks. The model is an effective theory approach that uses a non-local quark-hadron interaction Lagrangian and has a straightforward interpretation: the introduced interaction allows a hadron to turn into its constituent quarks which then interact according to the SM rules. The final state quarks are combined again to form outgoing hadrons. The model is constructed for various multiquark states, we use the meson formulation

$$\begin{aligned} \mathcal{L}_{\text{int}}^{\text{CCQM}}(x) &= g_M \cdot M_{(\mu)}(x) \cdot J_M^{(\mu)}(x), \\ J_M^{(\mu)}(x) &= \int dx_1 \int dx_2 F_M(x, x_1, x_2) \cdot \bar{q}_{f_1}^a(x_1) \Gamma_M^{(\mu)} q_{f_2}^a(x_2). \end{aligned}$$

Here the mesonic field M interacts with the quark current J_M with strength g_M . The symbol Γ_M represents an appropriate string of Dirac matrices to describe the spin of M and may carry a Lorentz index. Subscripts f denote flavors and superscripts a the color. We construct the vertex function F as

$$\begin{aligned} F_M(x, x_1, x_2) &= \delta(x - w_1 x_1 - w_2 x_2) \Phi_M \left[(x_1 - x_2)^2 \right], \\ w_i &= m_i / (m_1 + m_2), \end{aligned}$$

so that F is fully covariant and the hadron is positioned at the quark system's barycenter. The definition of Φ_M stands

$$\tilde{\Phi}_M(-k^2) = \exp(k^2/\Lambda_M^2) \quad (5)$$

and is guided also by the computational convenience. The symbol $\tilde{\Phi}$ denotes the Fourier transform into the momentum variable and the minus sign indicates that the Wick-rotated expression in the Euclidean space falls off quickly for integrals to be finite. The letter Λ represents a free model parameter linked to the meson

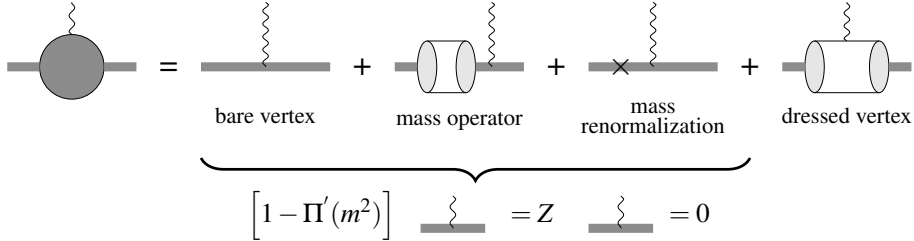


Figure 7: Diagrammatic representation of the compositeness condition.

M . Additional model parameters are constituent quark masses ($m_q = m_u = m_d$, m_s , m_c , m_b) and a cutoff parameter λ^{cutoff} needed to implement the confinement (see later).

There are few important principles that the CCQM incorporates in addition to the Lagrangian. First, as is evident from the construction above, mesonic and quark fields are present, both elementary. If the two fields can appear inside Feynman diagrams one worries about a possible double counting. Indeed, in nature, mesons and quarks are not independent but former are built from latter. We address this concern in a way described in [51, 52, 4], meaning that we apply the so-called compositeness condition

$$Z_M^{1/2} = 1 - 3g_M^2 \Pi_M'(m_M^2)/(4\pi) = 0, \quad (6)$$

where $Z_M^{1/2}$ is the meson renormalization constant and Π_M' is, for scalar mesons, the derivative of the meson mass operator. For vector mesons it is the derivative of the corresponding scalar par. Diagrammatically is (6) expressed in Fig. 7. The condition implies that the physical state has no overlap with the bare state, the interaction involves only constituents (quarks), which are however always virtual and therefore excluded from the space of physical parameters. The condition is satisfied by tuning the value of g_M . More details can be found for example in the section II of [2] and references therein.

An additional feature of the CCQM is the quark confinement that extends the model applicability to a hadron, whose mass exceeds the masses of its constituents summed. The approach is inspired by the confined-propagator technique which writes down the quark propagator in the Schwinger representation and introduces a cut in the integration limit

$$\frac{1}{m^2 - p^2} = \int_0^\infty d\alpha e^{-\alpha(m^2 - p^2)} \rightarrow \int_0^{1/\lambda^2} d\alpha e^{-\alpha(m^2 - p^2)} = \frac{1 - e^{-\frac{m^2 - p^2}{\lambda^2}}}{m^2 - p^2}.$$

The singularity for $p^2 \rightarrow m^2$ is removed for the expression on the right side, the propagator becomes an entire function without poles. The lack of singularities indicates an absence of asymptotic single-particle quark states, thus quarks are effectively confined. The procedure is for the CCQM more evolved (see Sec. II.c of [1]), the technique is applied to the whole structure of the Feynman

diagram F . Having n Schwinger parameters, one substitutes the unity in the form $1 = \int_0^\infty dt \delta(t - \sum_{i=1}^n \alpha_i)$ to get a product of an integration over a simplex and one improper integral

$$\begin{aligned}\Pi &= \int_0^\infty d^n \alpha F(\alpha_1, \dots, \alpha_n) \\ &= \int_0^{\infty \rightarrow \frac{1}{\lambda^2}} dt t^{n-1} \int_0^1 d^n \alpha \delta\left(t - \sum_{i=1}^n \alpha_i\right) F(t\alpha_1, \dots, t\alpha_n).\end{aligned}$$

The cut is applied to the one-dimensional integral only, but still, by analogous arguments, removes all existing thresholds in the quark-loop diagrams and provides a quark confinement. The cutoff parameter λ is a global model parameter.

Although we do not investigate radiative decays here, for completeness we mention that the model includes also interactions with photons: the free parts of the Lagrangian are gauged using the minimal subtraction procedure, and the gauge-field exponential technique is applied to the strong-interaction part, analogically to [53].

3.2 Application

The computations proceed by evaluation of relevant Feynman diagrams. The first step is the determination of the coupling g_M for all appearing mesons. This is done by applying the compositeness condition (6). Then one writes down the decay amplitude which is expressed as a product of a decay constant (or leptonic vector) and hadronic transition amplitude. The expression of the latter in the CCQM reads

$$\begin{aligned}(P'P)_V &= N_c g_P g_{P'} \int \frac{d^4 k}{(2\pi)^4 i} \tilde{\Phi}_P[-(k + w_{13}p_1)^2] \tilde{\Phi}_{P'}[-(k + w_{23}p_2)^2] \\ &\quad \times \text{tr} [O^\mu S_1(k + p_1) \gamma^5 S_3(k) \gamma^5 S_2(k + p_2)], \\(P'P)_S &= N_c g_P g_{P'} \int \frac{d^4 k}{(2\pi)^4 i} \tilde{\Phi}_P[-(k + w_{13}p_1)^2] \tilde{\Phi}_{P'}[-(k + w_{23}p_2)^2] \\ &\quad \times \text{tr} [S_1(k + p) \gamma^5 S_3(k) \gamma^5 S_2(k + p_2)], \\(VP)_V &= N_c g_P g_V \int \frac{d^4 k}{(2\pi)^4 i} \tilde{\Phi}_P[-(k + w_{13}p_1)^2] \tilde{\Phi}_V[-(k + w_{23}p_2)^2] \\ &\quad \times \text{tr} [O^\mu S_1(k + p_1) \gamma^5 S_3(k) \gamma^\nu (\epsilon_2^\dagger)_\nu S_2(k + p_2)], \\(VP)_T &= N_c g_P g_V \int \frac{d^4 k}{(2\pi)^4 i} \tilde{\Phi}_P[-(k + w_{13}p_1)^2] \tilde{\Phi}_V[-(k + w_{23}p_2)^2] \\ &\quad \times \text{tr} [\sigma^{\mu\nu} q_\nu (1 + \gamma^5) S_1(k + p_1) \gamma^5 S_3(k) \gamma^\nu (\epsilon_2^\dagger)_\nu S_2(k + p_2)],\end{aligned}\tag{7}$$

where N_c is the number of colors, $O^\mu = \gamma^\mu (1 - \gamma^5)$, S denotes the quark propagator and $w_{ij} = m_j / (m_i + m_j)$ with three contributing quarks. Indices $i = 1, 2$ label quarks in the decaying meson and $i = 2, 3$ in the final state meson, with

$i = 3$ being the spectator quark. Once these expressions are evaluated and compared to (4), the invariant form factors are extracted. For what concerns the calculations of leptonic decay constants and couplings g_M (the previously mentioned compositeness condition), they are similar and the corresponding CCQM expressions can be found for example in [2] (formulas 5 and 15 there). The above expressions are further processed: switching to the momentum picture an exponential appears, it contains exponents from the vertex function (5), from the Fourier-transformed propagators and also from the Schwinger parametrization. This exponent is then arranged by powers of k , formally written as $\exp(ak^2 + 2rk + z)$, and the loop momenta integral is evaluated thanks to the identity

$$\int d^4k P(k) e^{(ak^2 + 2rk + z)} = e^z P\left(\frac{1}{2} \frac{\partial}{\partial r}\right) \int d^4k e^{(ak^2 + 2rk)},$$

where a know Gaussian integral appears. Parameters a , r and z depend on Λ_P , $\Lambda_{P'}$ (or Λ_V), on α_i and on masses and external momenta, P denotes a polynomial from the trace evaluation. As a result, we get a polynomial built from a differential operator acting on an exponential in variable r . Again the computations are simplified using

$$P\left(\frac{1}{2} \frac{\partial}{\partial r}\right) e^{-\frac{r^2}{a}} = e^{-\frac{r^2}{a}} P\left(-\frac{r}{a} + \frac{1}{2} \frac{\partial}{\partial r}\right), \quad (8)$$

where the commutation makes the operator act on a unity. We extensively use the FORM [54] software, not only to evaluate the trace, but also for formal manipulations with the differential operator and commutations (8). The repeated use of the chain rule removes all derivatives from the expression and the integration over the Schwinger variables remains the last step before getting results

$$\Pi = \int_0^\infty d^n \alpha F(\alpha_1, \dots, \alpha_n).$$

Proceeding in accordance with the confinement implementation (Sec. 3.1), we perform a numerical integration using a Java numerical library [55].

4 Results

4.1 Numerical inputs

The values of Wilson coefficients evaluated at $\mu_b = 4.8$ GeV are taken from [56]. They stand

$$\begin{aligned} C_1 &= -0.2632, & C_2 &= 1.0111, & C_3 &= -0.0055, \\ C_4 &= -0.0806, & C_5 &= 0.0004, & C_6 &= 0.0009. \end{aligned}$$

We work in the large N_c limit $\xi \rightarrow 0$. The CCQM model inputs are represented by constituent quark masses (in GeV)

$$m_{u,d} = 0.241, \quad m_s = 0.428, \quad m_c = 1.672, \quad m_b = 5.046$$

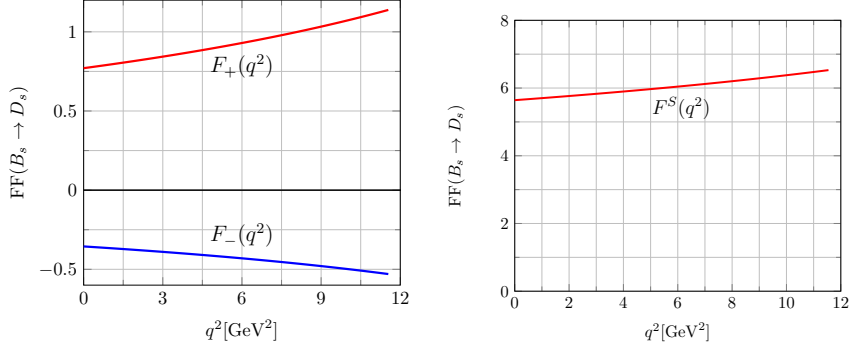


Figure 8: Form factors of the $B_s \rightarrow D_s$ transition.

and they were established in previous works by fitting the data. The same procedure was done for hadronic Λ parameters which are (in GeV)

$$\Lambda_{B_s} = 2.05, \Lambda_{D_s} = 1.75, \Lambda_\pi = 0.87, \Lambda_\rho = 0.61, \Lambda_\phi = 0.88, \Lambda_{\eta_c} = 3.97.$$

The cutoff parameter has a universal value $\lambda = 0.181$ GeV. The QCD quark masses are (in GeV) $\bar{m}_c = 1.27$, $\bar{m}_b = 4.68$ and $\bar{m}_t = 173.3$ (they enter the C_9^{eff} coefficient in semileptonic decays).

For reproducibility reasons let us state also values of nature constants. We use (masses in GeV)

$$\begin{aligned} m_{B_s} &= 5.366, & m_{D_s} &= 1.968, & m_\phi &= 1.019, \\ |V_{cb}| &= 0.041, & |V_{ud}| &= 0.9737, & |V_{us}| &= 0.225, \\ |V_{cs}| &= 0.987, & |V_{cd}| &= 0.224, & |V_{tb}V_{ts}^*| &= 0.041. \end{aligned}$$

4.2 Derived quantities

Using methods described earlier we derive, as basic outputs of the CCQM, the leptonic decay constants and hadronic transition form factors. The former are predicted to be (in GeV)

$$\begin{aligned} f_\pi &= 0.130, & f_\pi^S &= 0.250, \\ f_\rho &= 0.218, & f_{\eta_c} &= 0.627, \\ f_D &= 0.206, & f_D^S &= 0.794, \\ f_{J/\psi} &= 0.415. \end{aligned}$$

The behavior of form factors is shown in Figs 8 and 9.

4.3 Decay widths

Once the decay constants and form factors are evaluated, branching fractions can be determined: they represent observable quantities. We compare our results

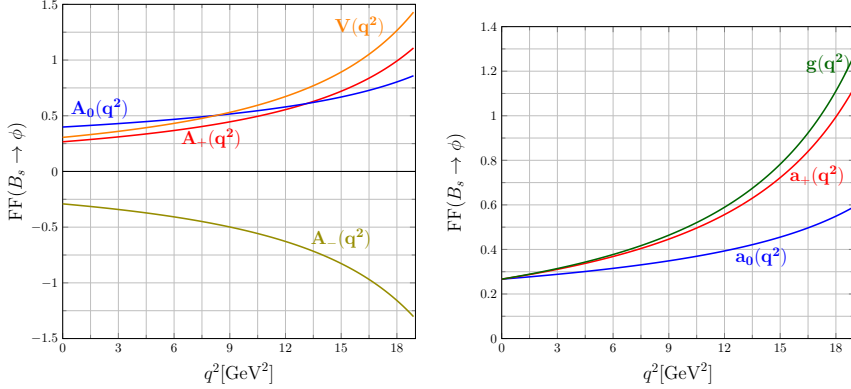


Figure 9: Form factors of the $B_s \rightarrow \phi$ transition.

to values published by the Particle Data Group (PDG) [8].

	CCQM	PDG
$\mathcal{B}(B_s^0 \rightarrow D_s^- \pi^+)$	5.107×10^{-3}	$(2.98 \pm 0.14) \times 10^{-3}$
$\mathcal{B}(B_s^0 \rightarrow D_s^- \rho^+)$	13.49×10^{-3}	$(6.8 \pm 1.4) \times 10^{-3}$
$\mathcal{B}(B_s^0 \rightarrow D_s^- D^+)$	4.89×10^{-4}	$(3.1 \pm 0.5) \times 10^{-4}$
$\mathcal{B}(B_s^0 \rightarrow K^- \pi^+)$	6.06×10^{-6}	$(5.9 \pm 0.7) \times 10^{-6}$
$\mathcal{B}(B_s^0 \rightarrow \phi \bar{D}^0)$	8.16×10^{-6}	$(23.0 \pm 2.5) \times 10^{-6}$
$\mathcal{B}(B_s^0 \rightarrow \phi \eta_c)$	12.89×10^{-4}	$(5.0 \pm 0.9) \times 10^{-4}$
$\mathcal{B}(B_s^0 \rightarrow \phi J/\psi)$	1.697×10^{-3}	$(1.03 \pm 0.04) \times 10^{-3}$
$\mathcal{B}(B_s^0 \rightarrow K^- D^+)$	9.376×10^{-7}	-
$\mathcal{B}(B_s^0 \rightarrow K^- D^{*+})$	9.930×10^{-7}	-
$\mathcal{B}(B_s^0 \rightarrow \phi D^0)$	1.362×10^{-6}	-
$\mathcal{B}(B_s^0 \rightarrow \phi \pi)$	1.555×10^{-8}	-
$\mathcal{B}(B_s^0 \rightarrow D_s^- \mu^+ \nu)$	2.697×10^{-2}	$(2.29 \pm 0.21) \times 10^{-2}$
$\mathcal{B}(B_s^0 \rightarrow K^- \mu^+ \nu)$	1.196×10^{-4}	$(1.06 \pm 0.09) \times 10^{-4}$
$\mathcal{B}(B_s^0 \rightarrow \phi^0 e^+ e^-)$	1.132×10^{-6}	-

As mentioned before, we crosscheck the $B_s^0 \rightarrow \phi J/\psi$ number above with our previous result from [5] where $\mathcal{B}(B_s^0 \rightarrow \phi J/\psi) = 1.6 \times 10^{-3}$. We see that our

model gives consistent results over time, yet, some small shifts can be caused by modification of the CCQM parameters when new global fits are done to determine them. The decay $B_s^0 \rightarrow \phi^0 e^+ e^-$ has no value for the total branching fraction, but numbers are known [17] for three individual q^2 intervals:

$10^8 \times \frac{\mathcal{B}(B_s^0 \rightarrow \phi^0 e^+ e^-)}{dq^2}$	q^2 interval (GeV)
CCQM	LHCb
6.12	13.8 ± 3.1 $0.1 < q^2 < 1.1$
3.30	2.6 ± 0.6 $0.1 < q^2 < 6.0$
4.88	3.9 ± 1.2 $15 < q^2 < 19$

5 Discussion, summary

The results give us a complex picture and one sees that for several decays the description of the data is bad. Before the quantitative comparison let us mention that the model has an intrinsic error and errors on its input parameters. It is difficult to provide a well justified estimate on how these impact the CCQM results: we attribute our predictions a fixed 25% uncertainty as a rough estimate. The errors were analyzed in details for different decays in [57] (section IV) and we consider the findings there as a justification for our choice, we do not perform a thorough analysis here. One may notice that the uncertainties established in [57] are larger than the ones previously used (see e.g references 53 and 54 of [57]).

The most precise results we get are represented by the semileptonic decays: here the description is fine. Even disregarding the model error the theoretical predictions are within the 2σ range of the experimental uncertainties.

A satisfactory agreement with the measured values is observed for $B_s^0 \rightarrow D_s^- D^+$ and $B_s^0 \rightarrow K^- \pi^+$, it is within acceptable error range when both, model and data errors are considered. These decays share the same diagrams but differ in form factors. The numbers are quite off for $B_s^0 \rightarrow D_s^- \pi^+$ and $B_s^0 \rightarrow D_s^- \rho^+$, approximately by a factor of 2. Relying on the theoretical uncertainty of 25% and adding errors in quadrature we get

$$B_s^0 \rightarrow D_s^- \pi^+ : |\mathcal{B}_{\text{CCQM}} - \mathcal{B}_{\text{Ex.}}| = (2.127 \pm 1.28) \times 10^{-3},$$

$$B_s^0 \rightarrow D_s^- \rho^+ : |\mathcal{B}_{\text{CCQM}} - \mathcal{B}_{\text{Ex.}}| = (6.69 \pm 3.65) \times 10^{-3}.$$

Clearly, our model error estimate is dominant and important when drawing a conclusion. If we trust it, we are at the limit of what can be accepted, with the deviations being close to 2σ , but not exceeding it. At this point a comparison with other authors becomes interesting. Most of them evaluate the charge-conjugated reaction.

Decay	Branching fraction $\times 10^3$	Source
$\bar{B}_s^0 \rightarrow D_s^+ \pi^-$	2.98 ± 0.14	Data (PDG)
	$2.8 \pm ?$	[23]
	$4.39_{-1.19}^{+1.36}$	[58]
	4.42 ± 0.21	[59]
	$4.61_{-0.39}^{+0.23}$	[22]
	$2.15_{-1.20}^{+2.14}$	[21]
$B_s^0 \rightarrow D_s^+ \rho^-$	6.8 ± 1.4	Data (PDG)
	$7.5 \pm ?$	[23]
	$11.30_{-3.11}^{+3.56}$	[58]

In general an overshooting of the experimental data is observed, which we confirm. The two works which give numbers near to experimental values have important errors: the number from [21] may be compatible with $\mathcal{B} \sim 4 \times 10^{-3}$ and the publication [23] does not provide uncertainties for the values we cite (Table 6b there). Yet, it provides errors for different decays (see e.g. Table 6a) and they are very important, reaching often 50-100%, even more. We therefore presume that the value 2.8×10^{-3} has also a very important error. When various models with different form factor derivation point in the same direction one may get the suspicion that the model itself cannot explain the discrepancies and that the decays are not well understood, some “physics” is missing. The authors of [59] even entitle it as a “puzzle”. It might be related to factorization breaking (see discussion in [59] and [21]), new physics [22] or some other effect.

From the three remaining decays that have experimental numbers, only the $B_s^0 \rightarrow \phi J/\psi$ is in rough agreement with the data

$$B_s^0 \rightarrow \phi J/\psi : |\mathcal{B}_{\text{CCQM}} - \mathcal{B}_{\text{Ex.}}| = (0.67 \pm 0.43) \times 10^{-3}.$$

Decays $B_s^0 \rightarrow \phi \bar{D}^0$ and $B_s^0 \rightarrow \phi \eta_c$ have significant deviations from measurements, and in opposite directions. Yet, they rely on the same form factor and share the color-suppressed diagram, complemented by a penguin in the η_c case. Again, comparison with other theoretical evaluations and their factorization approaches provides some insights (we do not distinguish between charge-conjugated modes)

$\mathcal{B}(B_s^0 \rightarrow \phi \bar{D}^0) \times 10^6$	Factorization	Source
23.0 ± 2.5		Data (PDG)
31 ± 7	Fact.-assisted topological-amplitude	[29]
0.873 ± 0.01	Naïve	[30]
$4.03^{+0.01}_{-0.02}$	QCD factorization (QCDF)	[30]
$5.47^{+1.01}_{-0.91}$	Final-state interactions (FSI)	[30]
$18.4^{+1.8}_{-1.7}$	QCDF+FSI	[30]
19.7 ± 4.5	Vertex + hard scatt. corr. (VHSC)	[31]

One sees that the authors of [30] tested various factorization techniques and got results which differ a lot. They reach the agreement with the data only when QCDF and FSI approaches are combined. The authors of [31] tested the scale dependence of the results for two methods (naïve, VHSC) and have shown an important scale dependence of the former, which is much less pronounced in the VHSC case. Including our result, we cannot get a fully coherent picture of the cause of existing variations but the conclusion that the naïve factorization we use is inappropriate seems plausible. Besides questioning the theoretical evaluations, it is also appropriate to point to the experimental situation: the LHCb number has changed significantly, at the limit of consistency [60, 13]

$$\mathcal{B}_{2018}^{\text{LHCb}} = (30.0 \pm 4.1) \times 10^{-6}, \quad \mathcal{B}_{2023}^{\text{LHCb}} = (23.0 \pm 2.5) \times 10^{-6}$$

Thus an additional experimental confirmation of the number is desirable before final conclusions are drawn.

The existing estimates for $B_s^0 \rightarrow \phi \eta_c$ stand

$\mathcal{B}(B_s^0 \rightarrow \phi \eta_c) \times 10^4$	Source
5.0 ± 0.9	Data (PDG)
2.795 ± 1.652	[32]
$5.63^{+1.86}_{-1.38}$	[33]

For this decay the published results are quite consistent with the experiment, but small in number. It is therefore difficult to identify the relevant differences that influence the result. The two displayed works use different factorization approaches (naïve vs. perturbative QCD) but also different ways for hadronic transition amplitudes.

At last, we want to mention the work [61], where the CCQM is used to describe nonleptonic decays of baryons. The authors take into the account long-distance interactions through pole diagrams which include intermediate

baryon resonances. They conclude that the pole diagrams are important to get consistency with measured data and this suggests that description of nonleptonic decays without these effects is not accurate enough.

In summary, we have in our work covered a wide area of B_s decay processes with various levels of agreement with data. We believe that a large part of inconsistencies can be attributed to the naïve factorization breaking. The B_s decays are often seen as complementary to the B_d ones. One can then follow the discussion regarding the factorization for $B_d \rightarrow DX$, which sometimes yields contradictory conclusions, e.g. [62] and [63]. Nevertheless, the processes $B_s^0 \rightarrow D_s^- \pi^+$ and $B_s^0 \rightarrow D_s^- \rho^+$ are among the cleanest non-leptonic decays with no penguin or color-suppressed contributions. Yet, systematic discrepancies are observed across several models, confirmed also by us. This is an interesting observation that deserves focus and additional analysis.

References

- [1] T. Branz, A. Faessler, T. Gutsche, M. A. Ivanov, J. G. Korner, and V. E. Lyubovitskij, “Relativistic constituent quark model with infrared confinement,” *Phys. Rev. D*, vol. 81, p. 034010, 2010.
- [2] M. A. Ivanov, J. G. Korner, S. G. Kovalenko, P. Santorelli, and G. G. Saidullaeva, “Form factors for semileptonic, nonleptonic and rare B (B_s) meson decays,” *Phys. Rev. D*, vol. 85, p. 034004, 2012.
- [3] S. Dubnicka, A. Z. Dubnickova, M. A. Ivanov, and A. Liptaj, “Decays $B_s \rightarrow J/\psi + \eta$ and $B_s \rightarrow J/\psi + \eta'$ in the framework of covariant quark model,” *Phys. Rev. D*, vol. 87, p. 074201, 2013.
- [4] A. Issadykov, M. A. Ivanov, and S. K. Sakhiyev, “Form factors of the B - S -transitions in the covariant quark model,” *Phys. Rev. D*, vol. 91, no. 7, p. 074007, 2015.
- [5] S. Dubnička, A. Z. Dubničková, A. Issadykov, M. A. Ivanov, A. Liptaj, and S. K. Sakhiyev, “Decay $B_s \rightarrow \phi \ell^+ \ell^-$ in covariant quark model,” *Phys. Rev. D*, vol. 93, no. 9, p. 094022, 2016.
- [6] S. Dubnička, A. Z. Dubničková, M. A. Ivanov, A. Liptaj, P. Santorelli, and C. T. Tran, “Study of $B_s \rightarrow \ell^+ \ell^- \gamma$ decays in covariant quark model,” *Phys. Rev. D*, vol. 99, no. 1, p. 014042, 2019.
- [7] A. Issadykov and M. A. Ivanov, “b-s Anomaly Decays in Covariant Quark Model,” *Phys. Part. Nucl. Lett.*, vol. 15, no. 4, pp. 393–396, 2018.
- [8] S. Navas *et al.*, “Review of particle physics,” *Phys. Rev. D*, vol. 110, no. 3, p. 030001, 2024. 2025 update: <https://pdglive.lbl.gov> (Accessed on 03.11.2025).

- [9] R. Aaij *et al.*, “Precise measurement of the f_s/f_d ratio of fragmentation fractions and of B_s^0 decay branching fractions,” *Phys. Rev. D*, vol. 104, no. 3, p. 032005, 2021.
- [10] R. Louvot *et al.*, “Observation of $B_s^0 \rightarrow D_s^{*-} \pi^+$, $B_s^0 \rightarrow D_s^{(*)-} \rho^+$ Decays and Measurement of $B_s^0 \rightarrow D_s^{*-} \rho^+$ Polarization,” *Phys. Rev. Lett.*, vol. 104, p. 231801, 2010.
- [11] R. Aaij *et al.*, “Study of beauty hadron decays into pairs of charm hadrons,” *Phys. Rev. Lett.*, vol. 112, p. 202001, 2014.
- [12] R. Aaij *et al.*, “Measurement of b -hadron branching fractions for two-body decays into charmless charged hadrons,” *JHEP*, vol. 10, p. 037, 2012.
- [13] R. Aaij *et al.*, “Evidence for the decays $B^0 \bar{B} \bar{D}^{(*)0} \phi$ and updated measurements of the branching fractions of the $B_s^0 \bar{B} \bar{D}^{(*)0} \phi$ decays,” *JHEP*, vol. 10, p. 123, 2023.
- [14] R. Aaij *et al.*, “Observation of the decay $B_s^0 \rightarrow \eta_c \phi$ and evidence for $B_s^0 \rightarrow \eta_c \pi^+ \pi^-$,” *JHEP*, vol. 07, p. 021, 2017.
- [15] R. Aaij *et al.*, “Measurement of $|V_{cb}|$ with $B_s^0 \rightarrow D_s^{(*)-} \mu^+ \nu_\mu$ decays,” *Phys. Rev. D*, vol. 101, no. 7, p. 072004, 2020.
- [16] R. Aaij *et al.*, “First observation of the decay $B_s^0 \rightarrow K^- \mu^+ \nu_\mu$ and Measurement of $|V_{ub}|/|V_{cb}|$,” *Phys. Rev. Lett.*, vol. 126, no. 8, p. 081804, 2021.
- [17] R. Aaij *et al.*, “Test of Lepton Flavor Universality with $B s^0 \bar{B} \phi \ell + \ell^-$ Decays,” *Phys. Rev. Lett.*, vol. 134, no. 12, p. 121803, 2025.
- [18] R. Aaij *et al.*, “Constraints on the photon polarisation in $b \bar{B} s \gamma$ transitions using $B_s^0 \bar{B} \phi e^+ e^-$ decays,” *JHEP*, vol. 03, p. 047, 2025.
- [19] R. Aaij *et al.*, “Angular analysis of the decay $B_s^0 \rightarrow \phi e^+ e^-$,” 4 2025.
- [20] R. Fleischer, N. Serra, and N. Tuning, “Tests of Factorization and SU(3) Relations in B Decays into Heavy-Light Final States,” *Phys. Rev. D*, vol. 83, p. 014017, 2011.
- [21] M. L. Piscopo and A. V. Rusov, “Non-factorisable effects in the decays $\bar{B}_s^0 \rightarrow D_s^+ \pi^-$ and $\bar{B}^0 \rightarrow D^+ K^-$ from LCSR,” *JHEP*, vol. 10, p. 180, 2023.
- [22] F.-M. Cai, W.-J. Deng, X.-Q. Li, and Y.-D. Yang, “Probing new physics in class-I B-meson decays into heavy-light final states,” *JHEP*, vol. 10, p. 235, 2021.
- [23] A. Deandrea, N. Di Bartolomeo, R. Gatto, and G. Nardulli, “Two-body nonleptonic decays of B and B(s) mesons,” *Phys. Lett. B*, vol. 318, pp. 549–558, 1993.

- [24] M. Jung and S. Schacht, “Standard model predictions and new physics sensitivity in $B \rightarrow DD$ decays,” *Phys. Rev. D*, vol. 91, no. 3, p. 034027, 2015.
- [25] A. Ali, G. Kramer, Y. Li, C.-D. Lu, Y.-L. Shen, W. Wang, and Y.-M. Wang, “Charmless non-leptonic B_s decays to PP , PV and VV final states in the pQCD approach,” *Phys. Rev. D*, vol. 76, p. 074018, 2007.
- [26] H.-Y. Cheng and C.-K. Chua, “QCD Factorization for Charmless Hadronic B_s Decays Revisited,” *Phys. Rev. D*, vol. 80, p. 114026, 2009.
- [27] M. Gronau and J. L. Rosner, “The Role of $B_s \rightarrow K\pi$ in determining the weak phase γ ,” *Phys. Lett. B*, vol. 482, pp. 71–76, 2000.
- [28] Y. Yang, Z.-J. Lu, S.-P. Jin, and J. Sun, “Revisiting $B_s \rightarrow PP$ and PV decays with contributions from ϕ_{B2} with the perturbative QCD approach,” *Eur. Phys. J. C*, vol. 85, no. 5, p. 544, 2025.
- [29] S.-H. Zhou, Y.-B. Wei, Q. Qin, Y. Li, F.-S. Yu, and C.-D. Lu, “Analysis of Two-body Charmed B Meson Decays in Factorization-Assisted Topological-Amplitude Approach,” *Phys. Rev. D*, vol. 92, no. 9, p. 094016, 2015.
- [30] M. R. Talebtash, A. Asadi, and H. Mehraban, “Analysis of the $B_s \rightarrow \bar{D}^0\phi$ decay,” *Eur. Phys. J. Plus*, vol. 131, no. 9, p. 312, 2016.
- [31] N. Bakhshi, A. Abdi Saray, and B. Mohammadi, “Study of Strange Beauty Neutral Meson Decays into $\bar{D}^{*0}(\bar{D}^0)$ and ϕ Mesons,” *Phys. Atom. Nucl.*, vol. 87, no. 6, pp. 815–821, 2024.
- [32] H.-W. Ke and X.-Q. Li, “Determining the effective Wilson coefficient a_2 in terms of $BR(B_s \rightarrow \eta_c\phi)$ and evaluating $BR(B_s \rightarrow \eta_c f_0(980))$,” *Phys. Rev. D*, vol. 96, no. 5, p. 053005, 2017.
- [33] Z.-J. Xiao, D.-C. Yan, and X. Liu, “ $B_{(s)} \rightarrow \eta_c(P, V)$ decays and effects of the next-to-leading order contributions in the perturbative QCD approach,” *Nucl. Phys. B*, vol. 953, p. 114954, 2020.
- [34] E. McLean, C. T. H. Davies, A. T. Lytle, and J. Koponen, “Lattice QCD form factor for $B_s \rightarrow D_s^* l \nu$ at zero recoil with non-perturbative current renormalisation,” *Phys. Rev. D*, vol. 99, no. 11, p. 114512, 2019.
- [35] M. Atoui, V. Morénas, D. Bećirevic, and F. Sanfilippo, “ $B_s \rightarrow D_s \ell \nu_\ell$ near zero recoil in and beyond the Standard Model,” *Eur. Phys. J. C*, vol. 74, no. 5, p. 2861, 2014.
- [36] E. McLean, C. T. H. Davies, J. Koponen, and A. T. Lytle, “ $B_s \rightarrow D_s \ell \nu$ Form Factors for the full q^2 range from Lattice QCD with non-perturbatively normalized currents,” *Phys. Rev. D*, vol. 101, no. 7, p. 074513, 2020.

[37] M. Bordone, N. Gubernari, D. van Dyk, and M. Jung, “Heavy-Quark expansion for $\bar{B}_s \rightarrow D_s^{(*)}$ form factors and unitarity bounds beyond the $SU(3)_F$ limit,” *Eur. Phys. J. C*, vol. 80, no. 4, p. 347, 2020.

[38] G. Martinelli, M. Naviglio, S. Simula, and L. Vittorio, “ $|V_{cb}|$, lepton flavor universality and $SU(3)_F$ symmetry breaking in $B_s \rightarrow D_s^{(*)} \ell \nu \ell$ decays through unitarity and lattice QCD,” *Phys. Rev. D*, vol. 106, no. 9, p. 093002, 2022.

[39] B.-Y. Cui, Y.-K. Huang, Y.-M. Wang, and X.-C. Zhao, “Shedding new light on $R(D(s)^{*})$ and $|V_{cb}|$ from semileptonic $B^-(s) \rightarrow D(s)^{*} \ell \nu^- \ell$ decays,” *Phys. Rev. D*, vol. 108, no. 7, p. L071504, 2023.

[40] C. M. Bouchard, G. P. Lepage, C. Monahan, H. Na, and J. Shigemitsu, “ $B_s \rightarrow K \ell \nu$ form factors from lattice QCD,” *Phys. Rev. D*, vol. 90, p. 054506, 2014.

[41] J. M. Flynn, T. Izubuchi, T. Kawanai, C. Lehner, A. Soni, R. S. Van de Water, and O. Witzel, “ $B \rightarrow \pi \ell \nu$ and $B_s \rightarrow K \ell \nu$ form factors and $|V_{ub}|$ from 2+1-flavor lattice QCD with domain-wall light quarks and relativistic heavy quarks,” *Phys. Rev. D*, vol. 91, no. 7, p. 074510, 2015.

[42] S. González-Solís, P. Masjuan, and C. Rojas, “Padé approximants to $B \rightarrow \pi \ell \nu \ell$ and $B_s \rightarrow K \ell \nu \ell$ and determination of $|V_{ub}|$,” *Phys. Rev. D*, vol. 104, no. 11, p. 114041, 2021.

[43] J. M. Flynn, R. C. Hill, A. Jüttner, A. Soni, J. T. Tsang, and O. Witzel, “Exclusive semileptonic $B_s \rightarrow K \ell \nu \ell$ decays on the lattice,” *Phys. Rev. D*, vol. 107, no. 11, p. 114512, 2023.

[44] T. Aaltonen *et al.*, “Measurement of the Forward-Backward Asymmetry in the $B \rightarrow K^{(*)} \mu^+ \mu^-$ Decay and First Observation of the $B_s^0 \rightarrow \phi \mu^+ \mu^-$ Decay,” *Phys. Rev. Lett.*, vol. 106, p. 161801, 2011.

[45] R. Aaij *et al.*, “Angular analysis and differential branching fraction of the decay $B_s^0 \rightarrow \phi \mu^+ \mu^-$,” *JHEP*, vol. 09, p. 179, 2015.

[46] A. Bharucha, D. M. Straub, and R. Zwicky, “ $B \rightarrow V \ell^+ \ell^-$ in the Standard Model from light-cone sum rules,” *JHEP*, vol. 08, p. 098, 2016.

[47] G. Buchalla, A. J. Buras, and M. E. Lautenbacher, “Weak decays beyond leading logarithms,” *Rev. Mod. Phys.*, vol. 68, pp. 1125–1144, 1996.

[48] M. Misiak, “The $b \rightarrow se^+e^-$ and $b \rightarrow s\gamma$ decays with next-to-leading logarithmic QCD corrections,” *Nucl. Phys. B*, vol. 393, pp. 23–45, 1993. [Erratum: Nucl.Phys.B 439, 461–465 (1995)].

[49] H. H. Asatryan, H. M. Asatrian, C. Greub, and M. Walker, “Calculation of two loop virtual corrections to $b \rightarrow sl^+l^-$ in the standard model,” *Phys. Rev. D*, vol. 65, p. 074004, 2002.

[50] M. A. Ivanov, J. G. Korner, and P. Santorelli, “Exclusive semileptonic and nonleptonic decays of the B_c meson,” *Phys. Rev. D*, vol. 73, p. 054024, 2006.

[51] A. Salam, “Lagrangian theory of composite particles,” *Nuovo Cim.*, vol. 25, pp. 224–227, 1962.

[52] S. Weinberg, “Elementary particle theory of composite particles,” *Phys. Rev.*, vol. 130, pp. 776–783, 1963.

[53] J. Terning, “Gauging nonlocal Lagrangians,” *Phys. Rev. D*, vol. 44, no. 3, pp. 887–897, 1991.

[54] J. Kuipers, T. Ueda, J. A. M. Vermaasen, and J. Vollinga, “FORM version 4.0,” *Comput. Phys. Commun.*, vol. 184, pp. 1453–1467, 2013.

[55] N. T., “The Adaptive Sparse Grid Integration Project,” 2003. Available at: <http://www.torstennahm.de/java> (Accessed on 20.10.2025).

[56] S. Descotes-Genon, T. Hurth, J. Matias, and J. Virto, “Optimizing the basis of $B \rightarrow K^* ll$ observables in the full kinematic range,” *JHEP*, vol. 05, p. 137, 2013.

[57] A. Issadykov, M. A. Ivanov, D.-K. N. Nguyen, C.-T. Tran, A. Tyulemissova, and Z. Tyulemissov, “Revisiting radiative transitions of charmonium states in covariant confined quark model,” 9 2025. Accepted for publication in Physical Review D (as of October 2025), <https://doi.org/10.1103/g1sg-zvyx>.

[58] T. Huber, S. Kränkl, and X.-Q. Li, “Two-body non-leptonic heavy-to-heavy decays at NNLO in QCD factorization,” *JHEP*, vol. 09, p. 112, 2016.

[59] M. Bordone, N. Gubernari, T. Huber, M. Jung, and D. van Dyk, “A puzzle in $\bar{B}_{(s)}^0 \rightarrow D_{(s)}^{(*)+} \{\pi^-, K^-\}$ decays and extraction of the f_s/f_d fragmentation fraction,” *Eur. Phys. J. C*, vol. 80, no. 10, p. 951, 2020.

[60] R. Aaij *et al.*, “Observation of $B_s^0 \rightarrow \bar{D}^{*0} \phi$ and search for $B^0 \rightarrow \bar{D}^0 \phi$ decays,” *Phys. Rev. D*, vol. 98, no. 7, p. 071103, 2018.

[61] M. A. Ivanov, V. E. Lyubovitskij, and Z. Tyulemissov, “Study of the non-leptonic decay $\Xi c \rightarrow \Lambda c + \pi^-$ in the covariant confined quark model,” *Phys. Rev. D*, vol. 108, no. 7, p. 073002, 2023.

[62] M. Neubert and A. A. Petrov, “Comments on color suppressed hadronic B decays,” *Phys. Lett. B*, vol. 519, pp. 50–56, 2001.

[63] Z.-z. Xing, “Determining the factorization parameter and strong phase differences in $B \rightarrow D^{(*)} \pi$ decays,” *HEPNP*, vol. 26, pp. 100–103, 2002.